

Strange tribaryons

T. Fernández-Caramés⁽¹⁾, A. Valcarce⁽²⁾, H. Garcilazo⁽³⁾, and P. González⁽¹⁾

(1) *Dpto. de Física Teórica and IFIC*

Universidad de Valencia - CSIC, E-46100 Burjassot, Valencia, Spain

(2) *Grupo de Física Nuclear and IUFFyM*

Universidad de Salamanca, E-37008 Salamanca, Spain

(3) *Escuela Superior de Física y Matemáticas,*

Instituto Politécnico Nacional, Edificio 9,

07738 México D.F., Mexico

Abstract

We use two-body potentials derived from a constituent quark cluster model to analyze the bound-state problem of the ΣNN system. The observables of the two-body subsystems, NN and ΣN , are well reproduced. We do not find ΣNN bound states, but there are two attractive channels with a resonance close above the three-body threshold. These channels are the $(I, J) = (1, 1/2)$ and $(0, 1/2)$, their quantum numbers, widths and energy ordering consistent with the recently measured strange tribaryons from the ${}^4\text{He}(K_{\text{stopped}}^-, N)$ reactions in the KEK PS E471 experiment.

Pacs: 13.75.Ev, 12.39.Jh, 21.45.+v

I. INTRODUCTION

Recently an exotic tribaryon resonance $S^0(3115)$ has been measured using the stopped K^- absorption experiment, ${}^4\text{He}(K_{\text{stopped}}^-, p)$, at KEK-PS [1]. The proton energy distribution shows a monoenergetic peak, with a significance of 13σ , interpreted as the formation of a new kind of neutral tribaryon with isospin $I = 1$ and strangeness $S = -1$. The extracted mass and width of the state are $3117.0_{-4.4}^{+1.5}$ MeV and < 21 MeV, respectively, and its main decay mode is found to be ΣNN . The recent detailed analysis of the neutron spectrum in ${}^4\text{He}(K_{\text{stopped}}^-, n)$ [2] has made manifest a second monoenergetic peak assigned to the formation of another strange tribaryon $S^+(3140)$ with a significance of 3.7σ . The mass and width of this state are deduced to be $3140.5_{-0.8}^{+3.0}(\text{syst}) \pm 2.3(\text{stat})$ MeV and < 21.6 MeV, respectively, its main decay mode being $\Sigma^\pm NN$. The isospin of the state is assigned to be zero. The experimental determination of spin-parity of these strange tribaryons is awaited.

These experimental studies were motivated by the theoretical prediction of two deeply bound states in the $K^- {}^3\text{He}$ system [3]. However neither their predicted binding energies nor their isospin level ordering correspond to the measured tribaryons. Actually a $I = 0$ state was predicted as the deepest one with a mass of about 3195 MeV (the $I = 1$ state being 87 MeV above). These difficulties may be resolved by taking care of relativistic effects and by invoking an enhanced $\bar{K}N$ interaction and a strong spin-orbit interaction in the dense nuclear medium [4]. A similar isospin reversing problem is found with the results of the $SU(3)$ multiskirmion description of multibaryon systems [5]. This model predicts the $B = 3$ and $S = -1$ lighter resonance to be a $(I, J^\pi) = (0, 1/2^+)$ with an $I = 1$ excited state 40 MeV higher, both belonging to the 35^* -plet of flavor. Very recently, a nona-quark interpretation of the strange tribaryons has been suggested, identifying the $S^0(3115)$ as a member of flavor 27-plet with $(I, J) = (1, 1/2)$ or $(1, 3/2)$ and the $S^+(3140)$ as a member of flavor 10^* -plet with $(I, J) = (0, 3/2)$ or of flavor 35^* -plet with $(I, J) = (0, 1/2)$ [6].

In this work we study the possible existence of ΣNN positive parity bound states using two-body potentials derived from a constituent quark cluster model. For this purpose we follow the same procedure that we used in the past to study three-body systems made of N 's and Δ 's. The three-body calculations are performed using a truncated T -matrix approximation where the inputs of the three-body equations are the two-body t -matrices truncated such that the orbital angular momentum in the initial and final states is equal to zero. These two-body t -matrices, however, have been constructed taking into account the coupling to the $\ell = 2$ states due to the tensor force. This approximation in the case of the three-nucleon system, with the NN interaction taken as the Reid soft-core potential, leads to a triton binding energy which differs less than 1 MeV from the exact value [7,8]. In a first approach, like in our previous studies of the bound-state problem of the ΔNN , $\Delta\Delta N$, and $\Delta\Delta\Delta$ systems [9–11], we deal with real integral equations since we do not consider the imaginary terms arising from the coupling of baryon-baryon subsystems to lower mass channels, i.e., from the coupling of the ΣN subsystem to the ΛN channel. Then, in a second more complete study we consider the full $\Sigma NN - \Lambda NN$ system to check the effect of the coupling to Λ channels at the three-body level.

We use as basic framework for the baryon-baryon interactions the local potentials obtained from the constituent quark cluster model since this provides a consistent and universal treatment for all of them [12]. The paper is organized as follows. In Sec. II we provide a

brief description of the constituent quark model and the formalism to study the two and three-body systems. In Sec. III we present and discuss our results. Finally we summarize our main conclusions in Sec. IV.

II. FORMALISM

A. The two-body interactions

The baryon-baryon interactions involved in the study of the ΣNN system are obtained from the constituent quark cluster model [12,13]. In this model baryons are described as clusters of three interacting massive (constituent) quarks, the mass coming from the spontaneous breaking of chiral symmetry. The ingredients of the quark-quark interaction are confinement (CON), one-gluon (OGE), one-pion (π), one-sigma (σ), one-kaon (K) and one-eta (η) exchange terms. Explicitly, the quark-quark interaction reads:

$$V_{qq}(\vec{r}_{ij}) = V_{CON}(\vec{r}_{ij}) + V_{OGE}(\vec{r}_{ij}) + V_{\pi}(\vec{r}_{ij}) + V_{\sigma}(\vec{r}_{ij}) + V_K(\vec{r}_{ij}) + V_{\eta}(\vec{r}_{ij}) , \quad (1)$$

where the i and j indices are associated with i and j quarks respectively, \vec{r}_{ij} stands for the interquark distance and

$$V_{CON}(\vec{r}_{ij}) = -a_c \vec{\lambda}_i^c \cdot \vec{\lambda}_j^c r_{ij} , \quad (2)$$

$$V_{OGE}(\vec{r}_{ij}) = \frac{1}{4} \alpha_s \vec{\lambda}_i^c \cdot \vec{\lambda}_j^c \left\{ \frac{1}{r_{ij}} - \frac{1}{4} \left(\frac{1}{2m_i^2} + \frac{1}{2m_j^2} + \frac{2}{3m_i m_j} \vec{\sigma}_i \cdot \vec{\sigma}_j \right) \frac{e^{-r_{ij}/r_0}}{r_0^2 r_{ij}} \right\} , \quad (3)$$

$$\begin{aligned} V_{\pi}(\vec{r}_{ij}) = & \frac{1}{3} \frac{g_{ch}^2}{4\pi} \frac{m_{\pi}^2}{4m_i m_j} \frac{\Lambda_{\chi}^2}{\Lambda_{\chi}^2 - m_{\pi}^2} m_{\pi} \left\{ \left[Y(m_{\pi} r_{ij}) - \frac{\Lambda_{\chi}^3}{m_{\pi}^3} Y(\Lambda_{\chi} r_{ij}) \right] \vec{\sigma}_i \cdot \vec{\sigma}_j \right. \\ & \left. + \left[H(m_{\pi} r_{ij}) - \frac{\Lambda_{\chi}^3}{m_{\pi}^3} H(\Lambda_{\chi} r_{ij}) \right] S_{ij} \right\} \sum_{a=1}^3 (\lambda_i^a \cdot \lambda_j^a) , \end{aligned} \quad (4)$$

$$V_{\sigma}(\vec{r}_{ij}) = -\frac{g_{ch}^2}{4\pi} \frac{\Lambda_{\chi}^2}{\Lambda_{\chi}^2 - m_{\sigma}^2} m_{\sigma} \left[Y(m_{\sigma} r_{ij}) - \frac{\Lambda_{\chi}}{m_{\sigma}} Y(\Lambda_{\chi} r_{ij}) \right] , \quad (5)$$

$$\begin{aligned} V_K(\vec{r}_{ij}) = & \frac{1}{3} \frac{g_{ch}^2}{4\pi} \frac{m_K^2}{4m_i m_j} \frac{\Lambda_K^2}{\Lambda_K^2 - m_K^2} m_K \left\{ \left[Y(m_K r_{ij}) - \frac{\Lambda_K^3}{m_K^3} Y(\Lambda_K r_{ij}) \right] (\vec{\sigma}_i \cdot \vec{\sigma}_j) \right. \\ & \left. + \left[H(m_K r_{ij}) - \frac{\Lambda_K^3}{m_K^3} H(\Lambda_K r_{ij}) \right] S_{ij} \right\} \sum_{a=4}^7 (\lambda_i^a \cdot \lambda_j^a) , \end{aligned} \quad (6)$$

$$\begin{aligned} V_{\eta}(\vec{r}_{ij}) = & \frac{1}{3} \frac{g_{ch}^2}{4\pi} \frac{m_{\eta}^2}{4m_i m_j} \frac{\Lambda_{\eta}^2}{\Lambda_{\eta}^2 - m_{\eta}^2} m_{\eta} \left\{ \left[Y(m_{\eta} r_{ij}) - \frac{\Lambda_{\eta}^3}{m_{\eta}^3} Y(\Lambda_{\eta} r_{ij}) \right] (\vec{\sigma}_i \cdot \vec{\sigma}_j) \right. \\ & \left. + \left[H(m_{\eta} r_{ij}) - \frac{\Lambda_{\eta}^3}{m_{\eta}^3} H(\Lambda_{\eta} r_{ij}) \right] S_{ij} \right\} [\cos\theta_P(\lambda_i^{a=8} \cdot \lambda_j^{a=8}) - \sin\theta_P] , \end{aligned}$$

being

$$Y(x) = \frac{e^{-x}}{x} \quad ; \quad H(x) = \left(1 + \frac{3}{x} + \frac{3}{x^2}\right)Y(x). \quad (7)$$

a_c is the confinement strength, the $\vec{\lambda}^a$'s ($\vec{\lambda}^a$'s) are the $SU(3)$ color (flavor) matrices, α_s is an effective strong coupling constant, m_i is the mass of the quark i . $\vec{\sigma}_i$ stands for the Pauli spin operator, g_{ch} is the chiral coupling constant and Λ_i are cut-off parameters. m_π , m_σ , m_K and m_η are the masses of the exchanged bosons. The angle θ_P appears as a consequence of considering the physical η instead the octet one. Finally, S_{ij} is the usual quark-tensor operator $S_{ij} = 3(\vec{\sigma}_i \cdot \hat{r}_{ij})(\vec{\sigma}_j \cdot \hat{r}_{ij}) - \vec{\sigma}_i \cdot \vec{\sigma}_j$. The parameters of the model are those of Ref. [13].

In order to derive the local $NB_1 \rightarrow NB_2$ interactions ($B_i = N, \Delta, \Sigma, \Lambda$) from the basic qq interaction defined above we use a Born-Oppenheimer approximation. Explicitly, the potential is calculated as follows,

$$V_{NB_1(LST) \rightarrow NB_2(L'S'T)}(R) = \xi_{LST}^{L'S'T}(R) - \xi_{LST}^{L'S'T}(\infty), \quad (8)$$

where

$$\xi_{LST}^{L'S'T}(R) = \frac{\langle \Psi_{NB_2}^{L'S'T}(\vec{R}) | \sum_{i < j=1}^6 V_{qq}(\vec{r}_{ij}) | \Psi_{NB_1}^{LST}(\vec{R}) \rangle}{\sqrt{\langle \Psi_{NB_2}^{L'S'T}(\vec{R}) | \Psi_{NB_2}^{L'S'T}(\vec{R}) \rangle} \sqrt{\langle \Psi_{NB_1}^{LST}(\vec{R}) | \Psi_{NB_1}^{LST}(\vec{R}) \rangle}}. \quad (9)$$

In the last expression the quark coordinates are integrated out keeping R fixed, the resulting interaction being a function of the $N - B_i$ distance. The wave function $\Psi_{NB_i}^{LST}(\vec{R})$ for the two-baryon system is discussed in detail in Ref. [12].

B. The NN and ΣN subsystems

If we consider the system of two baryons N and B ($B = N, \Sigma, \Lambda$) in a relative S -state interacting through a potential V that contains a tensor force, then there is a coupling to the NB D -wave so that the Lippmann-Schwinger equation of the system is of the form

$$t_{ji}^{\ell s \ell' s''}(p, p''; E) = V_{ji}^{\ell s \ell' s''}(p, p'') + \sum_{\ell' s'} \int_0^\infty p'^2 dp' V_{ji}^{\ell s \ell' s'}(p, p') \\ \times \frac{1}{E - p'^2/2\mu + i\epsilon} t_{ji}^{\ell' s' \ell'' s''}(p', p''; E), \quad (10)$$

where t is the two-body amplitude, j , i , and E are the angular momentum, isospin and energy of the system, and ℓs , $\ell' s'$, $\ell'' s''$ are the initial, intermediate, and final orbital angular momentum and spin. p and μ are, respectively, the relative momentum and reduced mass of the two-body system. More precisely, Eq. (10) is only valid for the ΣN system with isospin 3/2 and the NN system with isospin 0. For these cases, the coupled channels of orbital angular momentum and spin that contribute are given in the first rows of Tables I and II, respectively.

In the case of the ΣN system with isospin $i = 1/2$, the ΣN states are coupled to ΛN states. Thus, if we denote the ΣN system as channel Σ and the ΛN system as channel Λ , instead of Eq. (10) the Lippmann-Schwinger equation for ΣN scattering with isospin $1/2$ becomes

$$t_{\alpha\beta;ji}^{\ell_\alpha s_\alpha \ell_\beta s_\beta}(p_\alpha, p_\beta; E) = V_{\alpha\beta;ji}^{\ell_\alpha s_\alpha \ell_\beta s_\beta}(p_\alpha, p_\beta) + \sum_{\gamma=\Sigma, \Lambda} \sum_{\ell_\gamma=0,2} \int_0^\infty p_\gamma^2 dp_\gamma V_{\alpha\gamma;ji}^{\ell_\alpha s_\alpha \ell_\gamma s_\gamma}(p_\alpha, p_\gamma) \\ \times G_\gamma(E; p_\gamma) t_{\gamma\beta;ji}^{\ell_\gamma s_\gamma \ell_\beta s_\beta}(p_\gamma, p_\beta; E); \quad \alpha, \beta = \Sigma, \Lambda \quad (11)$$

where $t_{\Sigma\Sigma;ji}$ is the $N\Sigma \rightarrow N\Sigma$ scattering amplitude, $t_{\Lambda\Lambda;ji}$ is the $N\Lambda \rightarrow N\Lambda$ scattering amplitude, and $t_{\Sigma\Lambda;ji}$ is the $N\Sigma \rightarrow N\Lambda$ scattering amplitude. The propagators $G_\Sigma(E; p_\Sigma)$ and $G_\Lambda(E; p_\Lambda)$ in Eq. (11) are given by

$$G_\Sigma(E; p_\Sigma) = \frac{2\mu_{N\Sigma}}{k_\Sigma^2 - p_\Sigma^2 + i\epsilon}, \quad (12)$$

$$G_\Lambda(E; p_\Lambda) = \frac{2\mu_{N\Lambda}}{k_\Lambda^2 - p_\Lambda^2 + i\epsilon}, \quad (13)$$

with

$$E = k_\Sigma^2/2\mu_{N\Sigma}, \quad (14)$$

where the on-shell momenta k_Σ and k_Λ are related by

$$\sqrt{m_N^2 + k_\Sigma^2} + \sqrt{m_\Sigma^2 + k_\Sigma^2} = \sqrt{m_N^2 + k_\Lambda^2} + \sqrt{m_\Lambda^2 + k_\Lambda^2}. \quad (15)$$

We give in Table I the channels (ℓ_Σ, s_Σ) and $(\ell_\Lambda, s_\Lambda)$ corresponding to the ΣN and ΛN systems that are coupled together for the isospin $1/2$ ΣN channels.

In the case of the NN system with isospin 1 we will take into account in an analogous manner the coupling between the NN and ΔN systems. If we denote the NN system as channel N and the ΔN system as channel Δ , then we shall write,

$$t_{\alpha\beta;ji}^{\ell_\alpha s_\alpha \ell_\beta s_\beta}(p_\alpha, p_\beta; E) = V_{\alpha\beta;ji}^{\ell_\alpha s_\alpha \ell_\beta s_\beta}(p_\alpha, p_\beta) + \sum_{\gamma=N, \Delta} \sum_{\ell_\gamma s_\gamma} \int_0^\infty p_\gamma^2 dp_\gamma V_{\alpha\gamma;ji}^{\ell_\alpha s_\alpha \ell_\gamma s_\gamma}(p_\alpha, p_\gamma) \\ \times G_\gamma(E; p_\gamma) t_{\gamma\beta;ji}^{\ell_\gamma s_\gamma \ell_\beta s_\beta}(p_\gamma, p_\beta; E); \quad \alpha, \beta = N, \Delta \quad (16)$$

where $t_{NN;ji}$ is the $NN \rightarrow NN$ scattering amplitude, $t_{\Delta\Delta;ji}$ is the $N\Delta \rightarrow N\Delta$ scattering amplitude, and $t_{N\Delta;ji}$ is the $NN \rightarrow N\Delta$ scattering amplitude. The propagators $G_N(E; p_N)$ and $G_\Delta(E; p_\Delta)$ in Eq. (16) are given by

$$G_N(E; p_N) = \frac{2\mu_{NN}}{k_N^2 - p_N^2 + i\epsilon}, \quad (17)$$

$$G_\Delta(E; p_\Delta) = \frac{2\mu_{N\Delta}}{k_\Delta^2 - p_\Delta^2 + i\epsilon}, \quad (18)$$

with

$$E = k_N^2/2\mu_{NN}, \quad (19)$$

where the on-shell momenta k_N and k_Δ are related by

$$2\sqrt{m_N^2 + k_N^2} = \sqrt{m_N^2 + k_\Delta^2} + \sqrt{m_\Delta^2 + k_\Delta^2}. \quad (20)$$

We give in Table II the channels (ℓ_N, s_N) and (ℓ_Δ, s_Δ) corresponding to the NN and ΔN systems that are coupled together for the isospin 1 1S_0 NN channel.

As mentioned before, for the solution of the three-body system we will use only the component of the t -matrix obtained from the solution of Eq. (10) with $\ell = \ell'' = 0$, and of Eqs. (11) and (16) with $\ell_\alpha = \ell_\beta = 0$. For that purpose we define the S -wave truncated amplitude which in the case of the ΣN system with isospin 3/2 and the NN system with isospin 0 is defined from the solution of Eq. (10) by

$$t_{k;si}(p, p''; E) \equiv t_{ji}^{0s0s''}(p, p''; E) \quad , \quad k = NN, \Sigma\Sigma; \quad (21)$$

and for the ΣN - ΛN system with isospin 1/2 and the NN system with isospin 1 is defined, respectively, from the solution of Eqs. (11) and (16) by

$$t_{k;si}(p, p''; E) \equiv t_{\alpha\beta;ji}^{0s_\alpha 0s_\beta}(p, p''; E) \quad , \quad k = \alpha\beta = NN, \Sigma\Sigma, \Sigma\Lambda, \Lambda\Sigma, \Lambda\Lambda. \quad (22)$$

C. The ΣNN system

The numerical solution of the bound-state problem in the case of the ΣNN system will be obtained using the same formalism used in Ref. [10] for the case of the $\Delta\Delta N$ system since in both cases one is dealing with a system with two identical particles and a third one which is different. The effects of the ΛN and ΔN channels are included in the calculation of the $N\Sigma$ and NN t -matrices, respectively, as indicated in Eqs. (11) and (16). Since we are going to apply this formalism to the ΣNN bound-state problem the two-body propagators G_Σ , G_N , and G_Δ given by Eqs. (12), (17), and (18) never blow up. Only the propagator G_Λ given by Eq. (13) blows up since the ΛN channel is open, so that

$$G_\Lambda(E; p_\Lambda) = \frac{2\mu_{N\Lambda}}{k_\Lambda^2 - p_\Lambda^2} - \pi i 2\mu_{N\Lambda} \delta(k_\Lambda^2 - p_\Lambda^2). \quad (23)$$

However, from Ref. [14] we expect the imaginary part of the propagator G_Λ contributing mainly to the width of the ΣNN states while having very little effect on their masses. Therefore, in order to calculate the masses of the states we will neglect the imaginary part of this propagator so that our calculations will be done taking only the real part, i.e.,

$$G_\Lambda(E; p_\Lambda) \equiv \frac{2\mu_{N\Lambda}}{k_\Lambda^2 - p_\Lambda^2}. \quad (24)$$

However, when calculating their widths the full propagator, Eq. (23), will be used.

If we restrict ourselves to the configurations where all three particles are in S -wave states, the Faddeev equations for the bound-state problem in the case of three baryons with total spin S and total isospin I are

$$T_{i;SI}^{s_i i_i}(p_i q_i) = \sum_{j \neq i} \sum_{s_j i_j} h_{ij;SI}^{s_i i_i s_j i_j} \frac{1}{2} \int_0^\infty q_j^2 dq_j \int_{-1}^1 d\cos\theta t_{i;s_i i_i}(p_i, p'_i; E - q_i^2/2\nu_i) \\ \times \frac{1}{E - p_j^2/2\mu_j - q_j^2/2\nu_j} T_{j;SI}^{s_j i_j}(p_j q_j), \quad (25)$$

where $t_{1;s_1 i_1}$ stands for the two-body NN amplitude, and $t_{2;s_2 i_2}$ and $t_{3;s_3 i_3}$ for the ΣN amplitudes. p_i is the momentum of the pair jk (with ijk an even permutation of 123) and q_i the momentum of particle i with respect to the pair jk . μ_i and ν_i are the corresponding reduced masses

$$\mu_i = \frac{m_j m_k}{m_j + m_k}, \quad (26)$$

$$\nu_i = \frac{m_i(m_j + m_k)}{m_i + m_j + m_k}. \quad (27)$$

The momenta p'_i and p_j in Eq. (25) are given by

$$p_i'^2 = q_j^2 + \frac{\mu_i^2}{m_k^2} q_i^2 + 2 \frac{\mu_i}{m_k} q_i q_j \cos\theta, \quad (28)$$

$$p_j^2 = q_i^2 + \frac{\mu_j^2}{m_k^2} q_j^2 + 2 \frac{\mu_j}{m_k} q_i q_j \cos\theta. \quad (29)$$

$h_{ij;SI}^{s_i i_i s_j i_j}$ are the spin-isospin coefficients

$$h_{ij;SI}^{s_i i_i s_j i_j} = (-)^{s_j + \sigma_j - S} \sqrt{(2s_i + 1)(2s_j + 1)} W(\sigma_j \sigma_k S \sigma_i; s_i s_j) \\ \times (-)^{i_j + \tau_j - I} \sqrt{(2i_i + 1)(2i_j + 1)} W(\tau_j \tau_k I \tau_i; i_i i_j), \quad (30)$$

where W is the Racah coefficient and σ_i , s_i , and S (τ_i , i_i , and I) are the spins (isospins) of particle i , of the pair jk , and of the three-body system.

Since the variable p_i in Eq. (25) [also in Eqs. (10), (11), and (16)] runs from 0 to ∞ it is convenient to make the transformation

$$x_i = \frac{p_i - b}{p_i + b}, \quad (31)$$

where the new variable x_i runs from -1 to 1 and b is a scale parameter. With this transformation Eq. (25) takes the form

$$T_{i;SI}^{s_i i_i}(x_i q_i) = \sum_{j \neq i} \sum_{s_j i_j} h_{ij;SI}^{s_i i_i s_j i_j} \frac{1}{2} \int_0^\infty q_j^2 dq_j \int_{-1}^1 d\cos\theta t_{i;s_i i_i}(x_i, x'_i; E - q_i^2/2\nu_i) \\ \times \frac{1}{E - p_j^2/2\mu_j - q_j^2/2\nu_j} T_{j;SI}^{s_j i_j}(x_j q_j). \quad (32)$$

Since in the amplitude $t_{i;s_i i_i}(x_i, x'_i; e)$ the variables x_i and x'_i run from -1 to 1 , one can expand this amplitude in terms of Legendre polynomials as

$$t_{i;s_i i_i}(x_i, x'_i; e) = \sum_{nr} P_n(x_i) \tau_{i;s_i i_i}^{nr}(e) P_r(x'_i), \quad (33)$$

where the expansion coefficients are given by

$$\tau_{i;s_i i_i}^{nr}(e) = \frac{2n+1}{2} \frac{2r+1}{2} \int_{-1}^1 dx_i \int_{-1}^1 dx'_i P_n(x_i) t_{i;s_i i_i}(x_i, x'_i; e) P_r(x'_i). \quad (34)$$

Applying expansion (33) in Eq. (32) one gets

$$T_{i;SI}^{s_i i_i}(x_i q_i) = \sum_n T_{i;SI}^{ns_i i_i}(q_i) P_n(x_i), \quad (35)$$

where $T_{i;SI}^{ns_i i_i}(q_i)$ satisfies the one-dimensional integral equation

$$T_{i;SI}^{ns_i i_i}(q_i) = \sum_{j \neq i} \sum_{ms_j i_j} \int_0^\infty dq_j A_{ij;SI}^{ns_i i_i ms_j i_j}(q_i, q_j; E) T_{j;SI}^{ms_j i_j}(q_j), \quad (36)$$

with

$$\begin{aligned} A_{ij;SI}^{ns_i i_i ms_j i_j}(q_i, q_j; E) &= h_{ij;SI}^{s_i i_i s_j i_j} \sum_r \tau_{i;s_i i_i}^{nr}(E - q_i^2/2\nu_i) \frac{q_j^2}{2} \\ &\times \int_{-1}^1 d\cos\theta \frac{P_r(x'_i) P_m(x_j)}{E - p_j^2/2\mu_j - q_j^2/2\nu_j}. \end{aligned} \quad (37)$$

The three amplitudes $T_{1;SI}^{ls_1 i_1}(q_1)$, $T_{2;SI}^{ms_2 i_2}(q_2)$, and $T_{3;SI}^{ns_3 i_3}(q_3)$ in Eq. (36) are coupled together. The number of coupled equations can be reduced, however, since two of the particles are identical. The reduction procedure for the case where one has two identical fermions has been described before [15,16] and will not be repeated here. With the assumption that particle 1 is the Σ and particles 2 and 3 are the nucleons, only the amplitudes $T_{1;SI}^{rs_1 i_1}(q_1)$ and $T_{2;SI}^{ms_2 i_2}(q_2)$ are independent from each other and they satisfy the coupled integral equations

$$T_{1;SI}^{rs_1 i_1}(q_1) = 2 \sum_{ms_2 i_2} \int_0^\infty dq_3 A_{13;SI}^{rs_1 i_1 ms_2 i_2}(q_1, q_3; E) T_{2;SI}^{ms_2 i_2}(q_3), \quad (38)$$

$$\begin{aligned} T_{2;SI}^{ms_2 i_2}(q_2) &= \sum_{ms_3 i_3} G \int_0^\infty dq_3 A_{23;SI}^{ms_2 i_2 ms_3 i_3}(q_2, q_3; E) T_{2;SI}^{ms_3 i_3}(q_3) \\ &+ \sum_{rs_1 i_1} \int_0^\infty dq_1 A_{31;SI}^{ns_2 i_2 rs_1 i_1}(q_2, q_1; E) T_{1;SI}^{rs_1 i_1}(q_1), \end{aligned} \quad (39)$$

with the identical-particle factor

$$G = (-1)^{1+\sigma_1+\sigma_3-s_2+\tau_1+\tau_3-i_2}, \quad (40)$$

with σ_1 (τ_1) and σ_3 (τ_3) standing for the spin (isospin) of the Σ and the N respectively.

Substitution of Eq. (38) into Eq. (39) yields an equation with only the amplitude T_2

$$T_{2;SI}^{ms_2 i_2}(q_2) = \sum_{ms_3 i_3} \int_0^\infty dq_3 K_{SI}^{ms_2 i_2 ms_3 i_3}(q_2, q_3; E) T_{2;SI}^{ms_3 i_3}(q_3), \quad (41)$$

where

$$K_{SI}^{ns_2i_2ms_3i_3}(q_2, q_3; E) = GA_{23;SI}^{ns_2i_2ms_3i_3}(q_2, q_3; E) + 2 \sum_{rs_1i_1} \int_0^\infty dq_1 \\ \times A_{31;SI}^{ns_2i_2rs_1i_1}(q_2, q_1; E) A_{13;SI}^{rs_1i_1ms_3i_3}(q_1, q_3; E). \quad (42)$$

In order to find the solutions of Eq. (42) we replace the integral by a sum applying a numerical integration quadrature [17]. In this way Eq. (42) becomes a set of homogeneous linear equations. This set of linear equations has solutions only if the determinant of the matrix of the coefficients (the Fredholm determinant) vanishes for certain energies. Thus, the procedure to find the bound states of the system consists simply in searching for the zeroes of the Fredholm determinant as a function of energy. We give in Table III the six ΣNN states characterized by total isospin and spin (I, J) that are possible as well as the two-body ΣN and $NN(\Sigma)$ (NN channels with Σ spectator) channels that contribute to each state.

Our method of solution of the three-body problem is based in the separable expansion (33) of the two-body t -matrices. We tested in Ref. [10] (see Table IV of this reference) the convergence of this expansion by considering the three-nucleon bound-state problem with the Reid soft-core potential in the truncated T -matrix approximation (two-channel calculation) [8]. Convergence is reached with $N = 10$ (N is the number of Legendre polynomials in the separable expansion) although a very reasonable result is obtained already with $N = 5$. In the calculations of this paper we use $N = 10$.

D. The $\Sigma NN - \Lambda NN$ system

The numerical procedure to solve the bound state problem of the $\Sigma NN - \Lambda NN$ system is the same as the one described in the previous section but considering the full propagator $G_\Lambda(E; p_\Lambda)$ in Eq. (23). Besides, when one includes in addition to the ΣNN states also the ΛNN states, Eq. (41) becomes a two-component equation, i.e.,

$$T_{2;SI}^{ns_2i_2}(q_2) = \begin{pmatrix} T_{2;SI;\Sigma}^{ns_2i_2}(q_2) \\ T_{2;SI;\Lambda}^{ns_2i_2}(q_2) \end{pmatrix}, \quad (43)$$

and the kernel of Eq. (41) is now a 2×2 matrix defined by Eq. (42) with

$$A_{23;SI}^{ns_2i_2ms_3i_3}(q_2, q_3; E) = \begin{pmatrix} A_{23;SI;\Sigma\Sigma}^{ns_2i_2ms_3i_3}(q_2, q_3; E) & A_{23;SI;\Sigma\Lambda}^{ns_2i_2ms_3i_3}(q_2, q_3; E) \\ A_{23;SI;\Lambda\Sigma}^{ns_2i_2ms_3i_3}(q_2, q_3; E) & A_{23;SI;\Lambda\Lambda}^{ns_2i_2ms_3i_3}(q_2, q_3; E) \end{pmatrix}, \quad (44)$$

$$A_{31;SI}^{ns_2i_2rs_1i_1}(q_2, q_1; E) = \begin{pmatrix} A_{31;SI;\Sigma N(\Sigma)}^{ns_2i_2rs_1i_1}(q_2, q_1; E) & A_{31;SI;\Sigma N(\Lambda)}^{ns_2i_2rs_1i_1}(q_2, q_1; E) \\ A_{31;SI;\Lambda N(\Sigma)}^{ns_2i_2rs_1i_1}(q_2, q_1; E) & A_{31;SI;\Lambda N(\Lambda)}^{ns_2i_2rs_1i_1}(q_2, q_1; E) \end{pmatrix}, \quad (45)$$

$$A_{13;SI}^{rs_1i_1ms_3i_3}(q_1, q_3; E) = \begin{pmatrix} A_{13;SI;N\Sigma}^{rs_1i_1ms_3i_3}(q_1, q_3; E) & 0 \\ 0 & A_{13;SI;N\Lambda}^{rs_1i_1ms_3i_3}(q_1, q_3; E) \end{pmatrix}, \quad (46)$$

where

$$A_{23;SI;\alpha\beta}^{ns_2i_2ms_3i_3}(q_2, q_3; E) = h_{23;SI}^{s_2i_2s_3i_3} \sum_r \tau_{2;s_2i_2;\alpha\beta}^{nr} (E - q_2^2/2\nu_2) \frac{q_3^2}{2} \\ \times \int_{-1}^1 d\cos\theta \frac{P_r(x'_2)P_m(x_3)}{E + \Delta E\delta_{\beta\Lambda} - p_3^2/2\mu_3 - q_3^2/2\nu_3 + i\epsilon}; \quad \alpha, \beta = \Sigma, \Lambda, \quad (47)$$

$$A_{31;SI;\alpha N(\beta)}^{ns_2i_2ms_1i_1}(q_2, q_1; E) = h_{31;SI}^{s_2i_2s_1i_1} \sum_r \tau_{3;s_2i_2;\alpha\beta}^{nr} (E - q_2^2/2\nu_2) \frac{q_1^2}{2} \\ \times \int_{-1}^1 d\cos\theta \frac{P_r(x'_3)P_m(x_1)}{E + \Delta E\delta_{\beta\Lambda} - p_1^2/2\mu_1 - q_1^2/2\nu_1 + i\epsilon}; \quad \alpha, \beta = \Sigma, \Lambda, \quad (48)$$

$$A_{13;SI;N\beta}^{ns_1i_1ms_3i_3}(q_1, q_3; E) = h_{13;SI}^{s_1i_1s_3i_3} \sum_r \tau_{1;s_1i_1;NN}^{nr} (E + \Delta E\delta_{\beta\Lambda} - q_1^2/2\nu_1) \frac{q_3^2}{2} \\ \times \int_{-1}^1 d\cos\theta \frac{P_r(x'_1)P_m(x_3)}{E + \Delta E\delta_{\beta\Lambda} - p_3^2/2\mu_3 - q_3^2/2\nu_3 + i\epsilon}; \quad \beta = \Sigma, \Lambda, \quad (49)$$

with the isospin and mass of particle 1 (the hyperon) being determined by the subindex β . The subindex $\alpha N(\beta)$ in Eq. (48) indicates a transition $\alpha N \rightarrow \beta N$ with a nucleon as spectator followed by a $NN \rightarrow NN$ transition with β as spectator and,

$$\tau_{i;s_ii_i;\alpha\beta}^{nr}(e) = \frac{2n+1}{2} \frac{2r+1}{2} \int_{-1}^1 dx_i \int_{-1}^1 dx'_i P_n(x_i) t_{i;s_ii_i;\alpha\beta}(x_i, x'_i; e) P_r(x'_i). \quad (50)$$

We give in Table III the six $\Sigma NN - \Lambda NN$ states characterized by total isospin and spin (I, J) that are possible as well as the two-body ΣN , ΛN , $NN(\Sigma)$ (NN channels with Σ spectator) and $NN(\Lambda)$ (NN channels with Λ spectator) channels that contribute to each state.

The energy shift ΔE , which is usually taken as $M_\Sigma - M_\Lambda$, will be chosen instead such that at the Σd threshold the momentum of the Λd system has the correct value in consistency with the two-body prescription of Eqs. (15) and (20). Thus, writing

$$E = \frac{k_\Sigma^2}{2\mu_{\Sigma d}}, \quad (51)$$

$$E + \Delta E = \frac{k_\Lambda^2}{2\mu_{\Lambda d}}, \quad (52)$$

where k_Σ and k_Λ are related by

$$\sqrt{m_d^2 + k_\Sigma^2} + \sqrt{m_\Sigma^2 + k_\Sigma^2} = \sqrt{m_d^2 + k_\Lambda^2} + \sqrt{m_\Lambda^2 + k_\Lambda^2}, \quad (53)$$

if one takes $E = 0$, Eqs. (51)-(53) lead to

$$\Delta E = \frac{[(m_\Sigma + m_d)^2 - (m_\Lambda + m_d)^2][(m_\Sigma + m_d)^2 - (m_\Lambda - m_d)^2]}{8\mu_{\Lambda d}(m_\Sigma + m_d)^2}. \quad (54)$$

Since the ΛNN channels are in the continuum one has to deal with the three-body singularities arising from these channels. Thus, we used in Eqs. (41) and (42) the rotated-contour prescription

$$q_i \rightarrow q_i e^{-i\phi}; \quad i = 1, 2, 3, \quad (55)$$

since we found out numerically that the Fredholm determinant does not depend on the contour-rotation angle ϕ .

III. RESULTS

We will start by presenting the predictions of our model for the NN and ΣN subsystems and afterwards we discuss the three-body system.

A. The two-body subsystems

As has been discussed in detail in Ref. [9] a precise description of the NN low-energy observables is obtained. For the case of the $^3S_1 - ^3D_1$ interaction the model gives the correct binding energy for the deuteron and a pretty nice description of the phase shifts (see Figs. 2 and 3 of Ref. [9]). For isospin 1 channels the coupling to the ΔN system leads to a satisfactory description of the NN 1S_0 phase shift. The slightly different tuning of the cut-off for the 1S_0 ($\Lambda_\chi = 4.38 \text{ fm}^{-1}$) and 3S_1 ($\Lambda_\chi = 4.28 \text{ fm}^{-1}$) partial waves resembles the different value of the σ -meson parameters used by the Bonn potential for the same channels, in order to achieve a precise description of the low-energy data for both partial waves [18].

We now turn to the available low-energy data on the ΣN scattering. There is only a small amount of relevant data corresponding to the total cross sections (and some differential cross sections) for $\Sigma^+ p \rightarrow \Sigma^+ p$, $\Sigma^- p \rightarrow \Sigma^- p$, $\Sigma^- p \rightarrow \Sigma^0 n$, and $\Sigma^- p \rightarrow \Lambda n$ reactions. It has been known for a long time [19] that the available data do not allow for a unique effective range analysis. This is due (apart from the large error bars) to the absence of truly low-energy cross sections. The lowest hyperon laboratory momentum is larger than $100 \text{ MeV}/c$, which means that the inverse of the scattering length, $1/a$, and the range term, $rk^2/2$, can be of the same order, leading to results for the scattering length and effective range that are not unique. This has been clearly illustrated in Ref. [20] using six models for the hyperon-nucleon interaction with different properties on a detailed level, but providing all of them with an equally good description of the scattering data.

In the case of processes of the type $\Sigma N \rightarrow \Sigma N$ the amplitudes obtained from Eqs. (10) and (11) are related to the effective-range parameters a and r as

$$t_{\Sigma\Sigma;si}^{00} = -\frac{1}{\pi\mu_{N\Sigma}} \frac{1}{1/a_{si} + r_{si}k_\Sigma^2/2 - ik_\Sigma}, \quad (56)$$

so that the cross section for a given isospin state is

$$\begin{aligned}\sigma^i &= \pi^3 \mu_{N\Sigma}^2 \left(3 |t_{\Sigma\Sigma;1i}^{00}|^2 + |t_{\Sigma\Sigma;0i}^{00}|^2 \right) \\ &= \frac{3\pi}{k_\Sigma^2 + (1/a_{1i} + r_{1i}k_\Sigma^2/2)^2} + \frac{\pi}{k_\Sigma^2 + (1/a_{0i} + r_{0i}k_\Sigma^2/2)^2},\end{aligned}\quad (57)$$

We have tuned the interaction to reproduce the different total scattering cross sections by using the set of parameters of Ref. [13] and adjusting the harmonic oscillator parameter of the baryon wave function. As expected from the calculation of the root mean square radius of strange baryons [21] a slightly larger value of b_s is needed ($b_s = 0.7$ fm). From the isospin cross sections (57) the physical channels are determined through,

$$\begin{aligned}\sigma_{\Sigma^+p} &= \sigma^{i=3/2}, \\ \sigma_{\Sigma^-p} &= \frac{1}{9}\sigma^{i=3/2} + \frac{4}{9}\sigma^{i=1/2}, \\ \sigma_{\Sigma^-p \rightarrow \Sigma^0 n} &= \frac{2}{9}\sigma^{i=3/2} + \frac{2}{9}\sigma^{i=1/2}.\end{aligned}\quad (58)$$

In the case of the process $\Sigma N \rightarrow \Lambda N$ it is necessary to include also the transition with $\ell = 2$ in the ΛN channel since in that channel one is far above threshold. Thus, in that case the cross section for isospin $i = 1/2$ is

$$\sigma^{1/2} = \pi^3 \mu_{N\Sigma} \mu_{N\Lambda} \frac{k_\Lambda}{k_\Sigma} \left(|t_{\Sigma\Lambda;01/2}^{00}|^2 + 3 |t_{\Sigma\Lambda;11/2}^{00}|^2 + 3 |t_{\Sigma\Lambda;11/2}^{02}|^2 \right), \quad (59)$$

and the cross section for the physical channel is

$$\sigma_{\Sigma^-p \rightarrow \Lambda n} = \frac{2}{3}\sigma^{1/2}. \quad (60)$$

Our results are plotted in Fig. 1, where a good agreement with the experimental data is observed. The low-energy parameters for the different channels are given in Table IV. These parameters are complex in the case of the isospin 1/2 channel due to the fact that the ΛN channel is open. A similar agreement for the scattering cross sections has been obtained in Ref. [24] by means of a quark-model based interaction within a resonating group method calculation. Our results are also similar to those obtained by means of effective field theory in next-to-leading order [25] or those based on the new Nijmegen soft-core OBE hyperon-nucleon potential [20].

B. The three-body system

As a test of the reliability of our model in the case of the three-baryon system we solved the NNN bound-state problem. We found a triton binding energy of 6.90 MeV. For comparison, we notice that the triton binding energy for the Reid-soft-core potential in the truncated T -matrix approximation is 6.58 MeV [10].

In Fig. 2 we have plotted the Fredholm determinant of the ΣNN system for the three isospin channels with $J = 1/2$ and $J = 3/2$ calculated as explained in Sec. II C. As can be seen there are no bound states. The $J = 3/2$ channels are either repulsive or they do not

show any structure, as it is the case of the $I = 2$ channel that remains always flat. For the $J = 1/2$ case the $I = 2$ channel is repulsive, while the $I = 1$ and $I = 0$ are attractive, the $I = 1$ being always more attractive than the $I = 0$. If the attraction of the model is increased both channels develop bound states (the energy ordering between them being preserved), while all the others remain repulsive, what points out to a resonance close above the three-body threshold. This is illustrated in Fig. 3 where we plotted the Fredholm determinant in a model with more attraction ($b_s = 0.6$ fm), which therefore would not reproduce the ΣN scattering cross sections of Fig. 1. As can be seen the $I = 2, J = 1/2$ case remains equally repulsive while the $I = 1$ presents a bound state near threshold. For the $I = 0$ state a resonance behavior close above the three-body threshold is deduced. This shows that the ordering of the $I = 0$ and $I = 1$ states with $J = 1/2$ is preserved, the $I = 1$ channel being always the lowest state. The order of the two attractive channels can be easily understood looking at Tables III and IV. All the attractive two-body channels in the NN and ΣN subsystems contribute to the $(I, J) = (1, 1/2)$ ΣNN state (the ΣN channels $^3S_1(I = 1/2)$ and $^1S_0(I = 3/2)$ and the $^3S_1(I = 0)$ NN channel), while the $(I, J) = (0, 1/2)$ state do not present contribution from two of them, the $^1S_0(I = 3/2)$ ΣN and specially the $^3S_1(I = 0)$ NN deuteron channel. Actually, the NN deuteron-like contribution plays an essential role in the binding of the triton [12] and hypertriton [26]. In this last case the presence of the Λ has the effect of reducing the NN attraction with respect to the deuteron case but the $\Lambda \leftrightarrow \Sigma$ conversion compensates this reduction and binds the system.

In Fig. 4 we have plotted the real part of the Fredholm determinant of the $\Sigma NN - \Lambda NN$ system for the three isospin channels with $J = 1/2$ and $J = 3/2$ calculated as explained in Sec. IID. The imaginary parts are very small and uninteresting except for the calculation of the widths as we will see later. As can be seen the inclusion of the ΛNN channels does not modify the order of the states, giving values for the Fredholm determinant very close to the ones of the previous model (Fig. 2). This shows that the effect of the coupling to the Λ channels is very small at the three-body level once the coupling to the Λ is included at the two-body level.

The pattern of our results coincides exactly with the observations in the $^4\text{He}(K_{\text{stopped}}^-, N)$ reactions. In particular, we find only two attractive S -wave channels, with the isospin and energy ordering corresponding to the experimental $S^0(3115)$ and $S^+(3140)$ states. We predict for them $J^\pi = 1/2^+$.

Let us remind that the understanding of these states as deeply bound kaonic nuclear systems [3] would assign the quantum numbers $J^\pi = 3/2^+, I = 0$ for the $S^0(3115)$ and $J^\pi = 1/2^-, I = 1$ for the $S^+(3140)$. If some relativistic effects and a medium-enhanced $\bar{K}N$ and spin-orbit interactions are taken into account, the ordering of the isospin channels is reversed to $J^\pi = 3/2^+, I = 1$ and $J^\pi = 1/2^+, I = 0$. The $SU(3)$ multiskirmion description [5] finds $J^\pi = 1/2^+$ for both states, but the opposite ordering between the isospin states with respect to our results and experiment. The nona-quark study of Ref. [6] makes use of a Gell-Mann-Okubo like mass formula to study the spectrum of $S = -1, -2, -3$ nona-quark states. The color magnetic interaction between quarks, together with the antisymmetrization of the wave function, favors small multiplets in flavor and spin which gives a natural explanation for the $I = 1$ state being the lowest state among the $S = -1$ tribaryons with $J = 1/2$. This leads to the natural explanation that the $I = 1$ state could be a member of the 27 -plet with $J^\pi = 1/2$, and the $I = 0$ state may be a member of the 10^* -plet with $J^\pi = 3/2$.

However other possible classifications that may give rise to $J^\pi = 3/2$ for the $S^0(3115)$ and the $S^+(3140)$ were also discussed.

C. Calculation of the widths

In Fig. 3 we have shown the Fredholm determinant in the case when there is a bound state in the $(I, J) = (1, 1/2)$ channel. As discussed in subsection IIC, the Fredholm determinant is real since we have dropped the imaginary part of the propagator $G_\Lambda(E; p_\Lambda)$ in Eq. (23). Near the bound state the Fredholm determinant has the form $D(E) = C(E - E_0)$ where C is a constant and E_0 is the energy of the bound state. If we now repeat the calculation using the full propagator $G_\Lambda(E; p_\Lambda)$ given by Eq. (23) the Fredholm determinant becomes complex. Near the bound state it has the form $D(E) = C[(E - E_0) + i\Gamma]$ so that $1/|D(E)|^2$ has the resonant shape

$$\frac{1}{|D(E)|^2} = \frac{1}{|C|^2 [(E - E_0)^2 + \Gamma^2]}, \quad (61)$$

which is also the shape exhibited by the cross section near a resonance ($\sigma(E) \propto 1/|D(E)|^2$). In Fig. 5 we show $1/|D(E)|^2$, from which we extract $\Gamma = 0.3$ MeV for the model without ΛNN channels and $\Gamma = 0.5$ MeV for the model with ΛNN channels. This state lies 80 MeV above the ΛNN threshold while the observed tribaryons lie at 120 MeV and 140 MeV, respectively, above the ΛNN threshold.

Since the state of Fig. 3 has a width of less than 1 MeV one can reasonably expect that the observed states which lie 40 and 60 MeV above it will have somewhat larger widths but certainly in agreement with the experimental result $\Gamma < 21$ MeV.

IV. CONCLUSIONS

We have studied the bound-state solutions of the ΣNN system by means of interactions derived from a constituent quark cluster model. The two-body interactions correctly reproduce the low-energy observables of the NN and ΣN subsystems. We have not found any ΣNN bound state. However, our results show that there are only two attractive S -wave channels, they are the $(I, J) = (1, 1/2)$ and $(0, 1/2)$, with a resonance close above the three-body threshold. The channel with $I = 1$ is always more attractive than that with $I = 0$. The isospin quantum numbers and the energy ordering correspond exactly to the recently measured strange tribaryons from the ${}^4\text{He}(K_{\text{stopped}}^-, N)$ reactions in the KEK PS E471 experiment. We predict quantum numbers $J^\pi = 1/2^+$ and small widths for the two reported strange tribaryon resonances. The awaited experimental determination of J^π can serve as a stringent test of our model dynamics against others.

ACKNOWLEDGMENTS

This work has been partially funded by Ministerio de Educación y Ciencia under Contract No. FPA2004-05616, by Junta de Castilla y León under Contract No. SA-104/04, by

COFAA-IPN (México) and by Oficina de Ciencia y Tecnología de la Comunidad Valenciana, Grupos 03/094 and GV05/276.

REFERENCES

- [1] T. Suzuki *et al.*, Phys. Lett. B **597**, 263 (2004).
- [2] T. Suzuki *et al.*, Nucl. Phys. A **754**, 375 (2005). M. Iwasaki *et al.*, nucl-ex/0310018.
- [3] Y. Akaishi and T. Yamazaki, Phys. Rev. C **65**, 044005 (2002).
- [4] Y. Akaishi, A. Doté, and T. Yamazaki, Phys. Lett. B **613**, 140 (2005).
- [5] C.L. Schat and N.N. Scoccola, Phys. Rev. D **62**, 074010 (2000); J.P. Garrahan, M. Schvellinger, and N.N. Scoccola, Phys. Rev. D **61**, 014001 (1999).
- [6] Y. Maezawa, T. Hatsuda, and S. Sasaki, Prog. Theor. Phys. **114**, 317 (2005).
- [7] E.P. Harper, Y.E. Kim, and A. Tubis, Phys. Rev. Lett. **28**, 1533 (1972).
- [8] G.H. Berthold, H. Zankel, L. Mathelitsch, and H. Garcilazo, Il Nuovo Cimento **93 A**, 89 (1986).
- [9] H. Garcilazo, F. Fernández, A. Valcarce, and R.D. Mota, Phys. Rev. C **56**, 84 (1997).
- [10] R.D. Mota, A. Valcarce, F. Fernández, and H. Garcilazo, Phys. Rev. C **59**, 46 (1999).
- [11] H. Garcilazo, A. Valcarce, and F. Fernández, Phys. Rev. C **60**, 044002 (1999).
- [12] A. Valcarce, H. Garcilazo, F. Fernández, and P. González, Rep. Prog. Phys. **68**, 965 (2005).
- [13] J. Vijande, F. Fernández, and A. Valcarce, J. Phys. G **31**, 481 (2005).
- [14] H. Garcilazo, J. Phys. G **23**, 1101 (1997).
- [15] I.R. Afnan and A.W. Thomas, Phys. Rev. C **10**, 109 (1974).
- [16] H. Garcilazo and T. Mizutani, *πNN Systems* (World Scientific, Singapore, 1990).
- [17] M. Abramowitz and I.A. Stegun, *Handbook of Mathematical Functions* (Dover, New York, 1972).
- [18] R. Machleidt, K. Holinde, and C. Elster, Phys. Rep. **149**, 1 (1987).
- [19] J.J. de Swart, M.M. Nagels, T.A. Rijken, and P.A. Verhoeven, Springer Tracts. Mod. Phys. **60**, 138 (1971).
- [20] Th.A. Rijken, V.G.J. Stoks, and Y. Yamamoto, Phys. Rev. C **59**, 21 (1999).
- [21] M. Furuichi, K. Shimizu, and S. Takeuchi, Phys. Rev. C **68**, 034001 (2003); A. Valcarce, H. Garcilazo, and J. Vijande, Phys. Rev. C **72**, 025206 (2005).
- [22] F. Eisele, H. Filthuth, W. Fölsch, V. Hepp, E. Leitner, and G. Zetch, Phys. Lett. **37**, 204 (1971).
- [23] R. Engelmann, H. Filthuth, V. Hepp, and E. Kluge, Phys. Lett. B **21**, 587 (1966).
- [24] Z.Y. Zhang, Y.W. Yu, P.N. Shen, L.R. Dai, A. Faessler, and U. Straüb, Nucl. Phys. A **625**, 59 (1997).
- [25] C.L. Korpa, A.E.L. Dieperink, and R.G.E. Timmermans, Phys. Rev. C **65**, 015208 (2001).
- [26] K. Miyagawa, H. Kamada, W. Glöckle, and V. Stoks, Phys. Rev. C **51**, 2905 (1995).

TABLES

TABLE I. ΣN channels (ℓ_Σ, s_Σ) and ΛN channels $(\ell_\Lambda, s_\Lambda)$ that contribute to a given ΣN state with isospin i and total angular momentum j .

i	j	(ℓ_Σ, s_Σ)	$(\ell_\Lambda, s_\Lambda)$
3/2	0	(0,0)	
3/2	1	(0,1),(2,1)	
1/2	0	(0,0)	(0,0)
1/2	1	(0,1),(2,1)	(0,1),(2,1)

TABLE II. NN channels (ℓ_N, s_N) and ΔN channels (ℓ_Δ, s_Δ) that are coupled together in the ${}^3S_1 - {}^3D_1$, and 1S_0 NN states.

NN state	i	j	(ℓ_N, s_N)	(ℓ_Δ, s_Δ)
${}^3S_1 - {}^3D_1$	0	1	(0,1),(2,1)	
1S_0	1	0	(0,0)	(2,2)

TABLE III. Two-body ΣN channels (i_Σ, s_Σ) , ΛN channels (i_Λ, s_Λ) , NN channels with Σ spectator $(i_{N(\Sigma)}, s_{N(\Sigma)})$, and NN channels with Λ spectator $(i_{N(\Lambda)}, s_{N(\Lambda)})$ that contribute to a given $\Sigma NN - \Lambda NN$ state with total isospin I and spin J .

I	J	(i_Σ, s_Σ)	(i_Λ, s_Λ)	$(i_{N(\Sigma)}, s_{N(\Sigma)})$	$(i_{N(\Lambda)}, s_{N(\Lambda)})$
0	1/2	(1/2,0),(1/2,1)	(1/2,0),(1/2,1)	(1,0)	(0,1)
1	1/2	(1/2,0),(3/2,0),(1/2,1),(3/2,1)	(1/2,0),(1/2,1)	(0,1),(1,0)	(1,0)
2	1/2	(3/2,0),(3/2,1)		(1,0)	
0	3/2	(1/2,1)	(1/2,1)		(0,1)
1	3/2	(1/2,1),(3/2,1)	(1/2,1)	(0,1)	
2	3/2	(3/2,1)			

TABLE IV. Low-energy scattering parameters (in fm) of the ΣN 1S_0 and 3S_1 channels for the states with total isospin $i = 1/2$ and $i = 3/2$.

	1S_0		3S_1	
	a_s	r_s	a_t	r_t
$i = 1/2$	$-1.24 + i0.08$	$-0.80 - i0.33$	$4.65 + i4.22$	$3.13 - i0.43$
$i = 3/2$	3.16	4.78	-0.72	-0.63

FIGURES

FIG. 1. Calculated ΣN and $\Sigma N \rightarrow \Lambda N$ total cross sections compared with experimental data. Experimental data in (a) and (b) are from Ref. [22] and in (c) and (d) from Ref. [23].

FIG. 2. Fredholm determinant for (a) $J = 1/2$ and (b) $J = 3/2$ ΣNN channels for the model giving the ΣN total cross sections of Fig. 1. The Σd continuum starts at $E = -2.225$ MeV, the deuteron binding energy obtained within our model.

FIG. 3. $J = 1/2$ ΣNN Fredholm determinant for a model with increased attraction as explained in the text.

FIG. 4. Real part of the Fredholm determinant for (a) $J = 1/2$ and (b) $J = 3/2$ $\Sigma NN - \Lambda NN$ channels for the model giving the ΣN total cross sections of Fig. 1. The Σd continuum starts at $E = -2.225$ MeV, the deuteron binding energy obtained within our model.

FIG. 5. Inverse of the square of the Fredholm determinant, $1/|D(E)|^2$, for the bound state case of Fig. 3, $(I, J) = (1, 1/2)$, using the full propagator $G_\Lambda(E; p_\Lambda)$ in Eq. (23) (dashed line) and considering also the ΛNN channels (solid line).

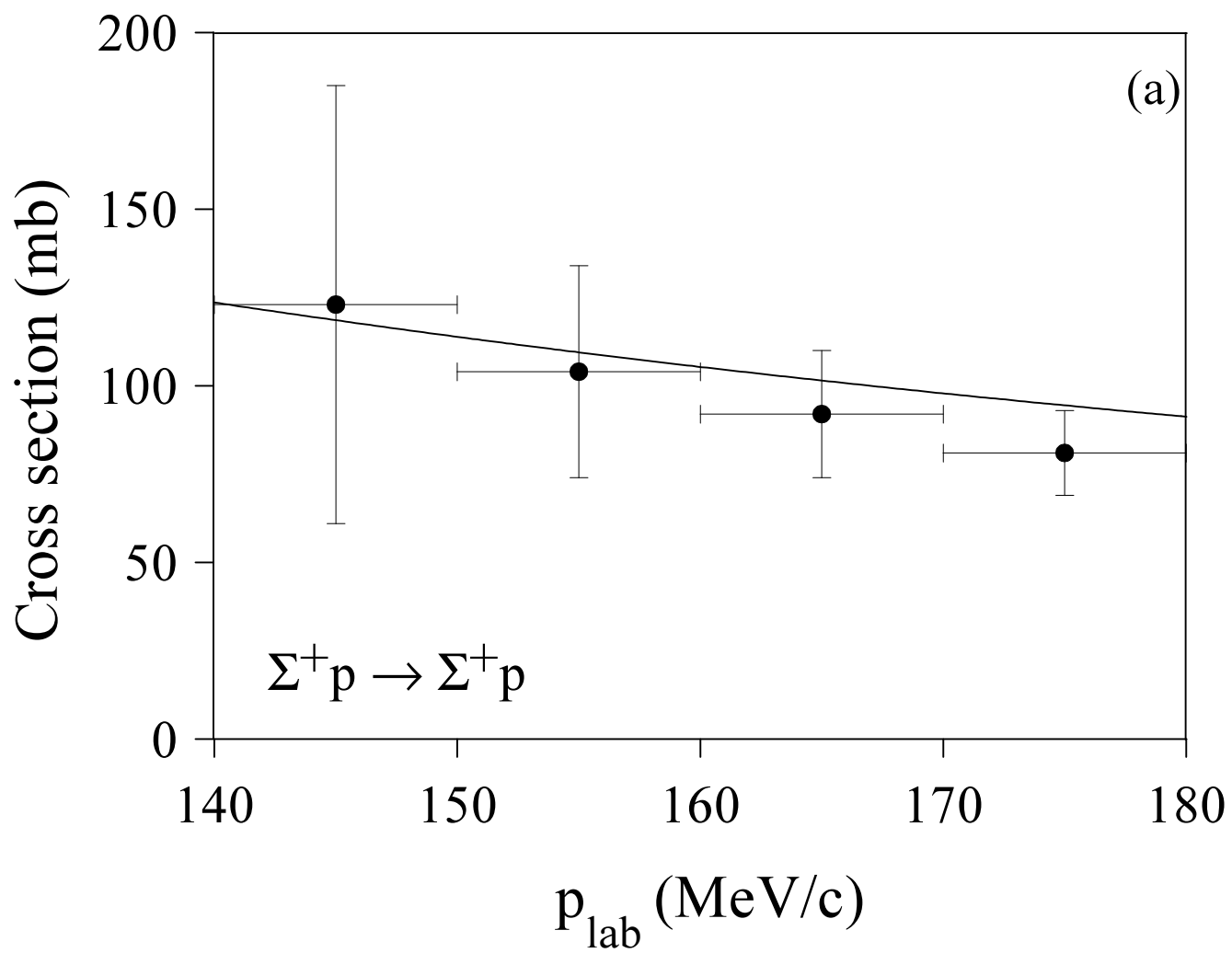


Figure 1

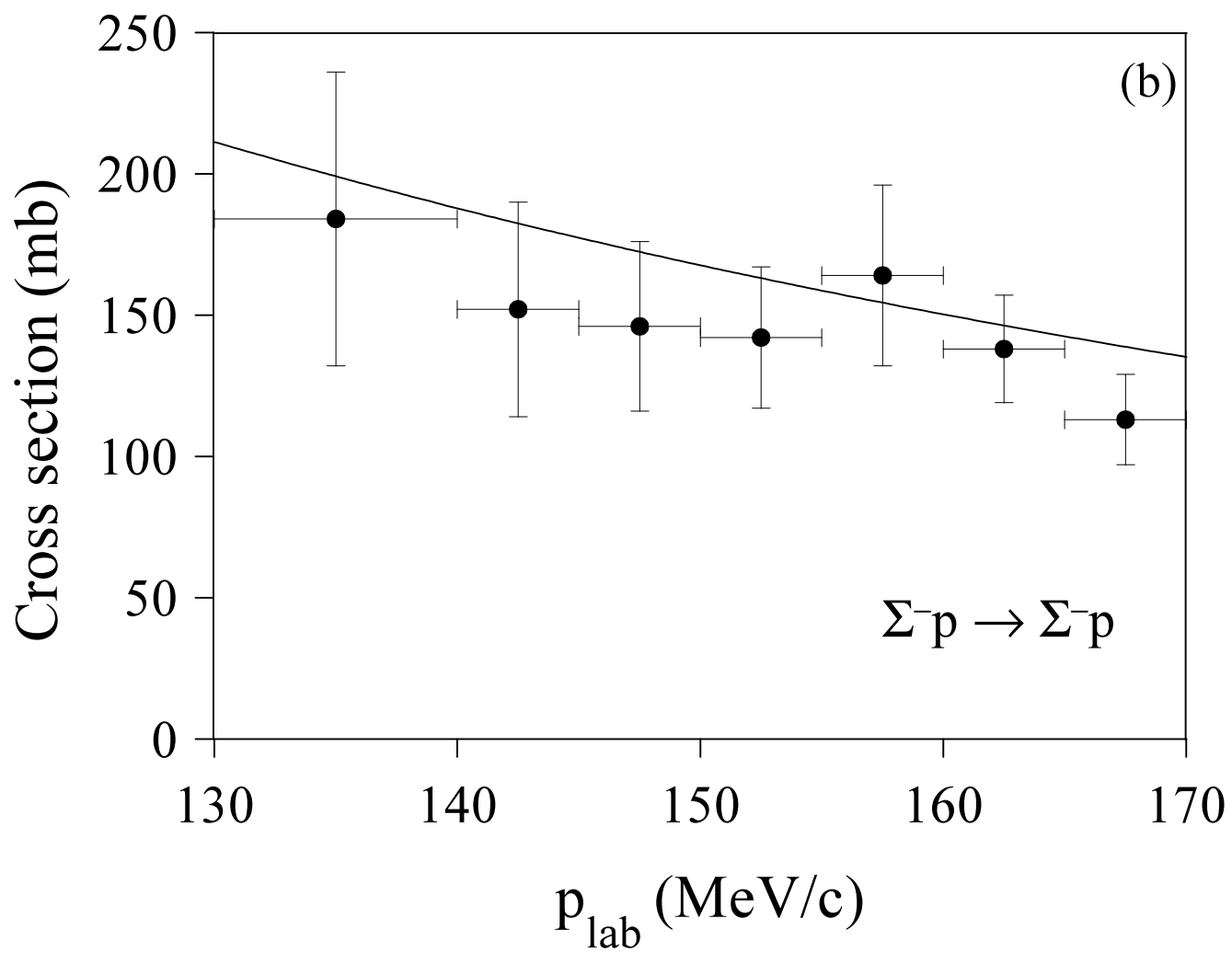


Figure 1

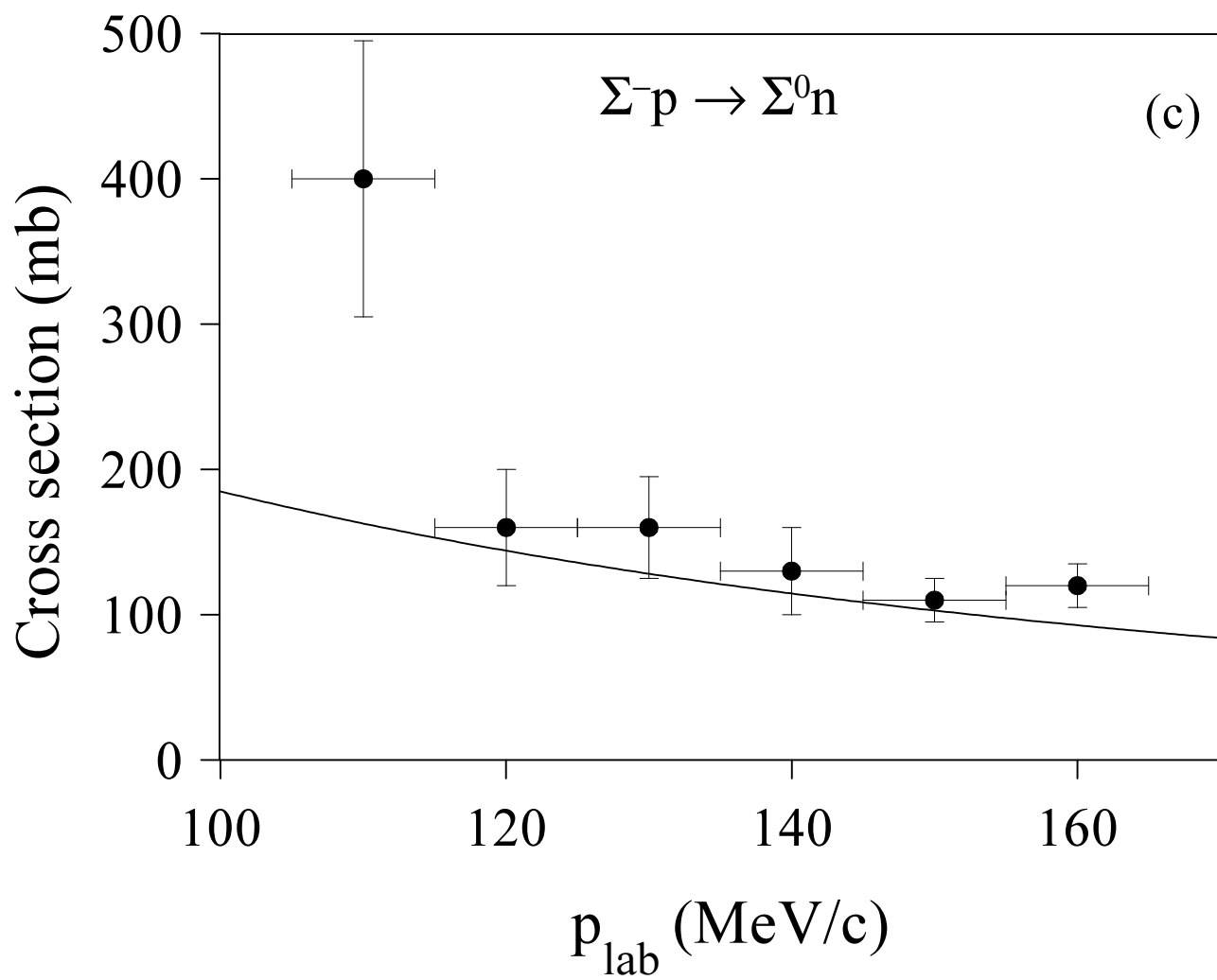


Figure 1

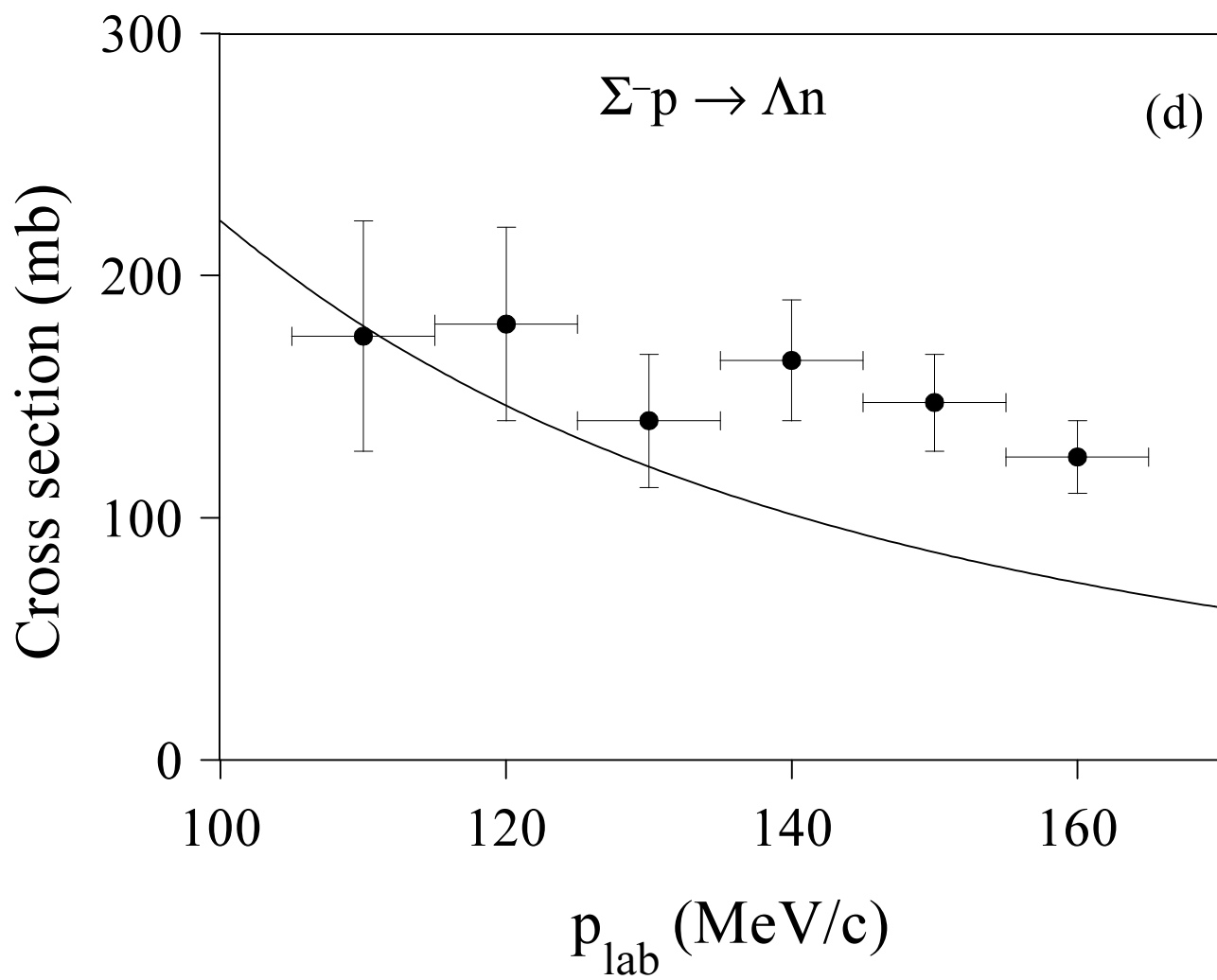


Figure 1

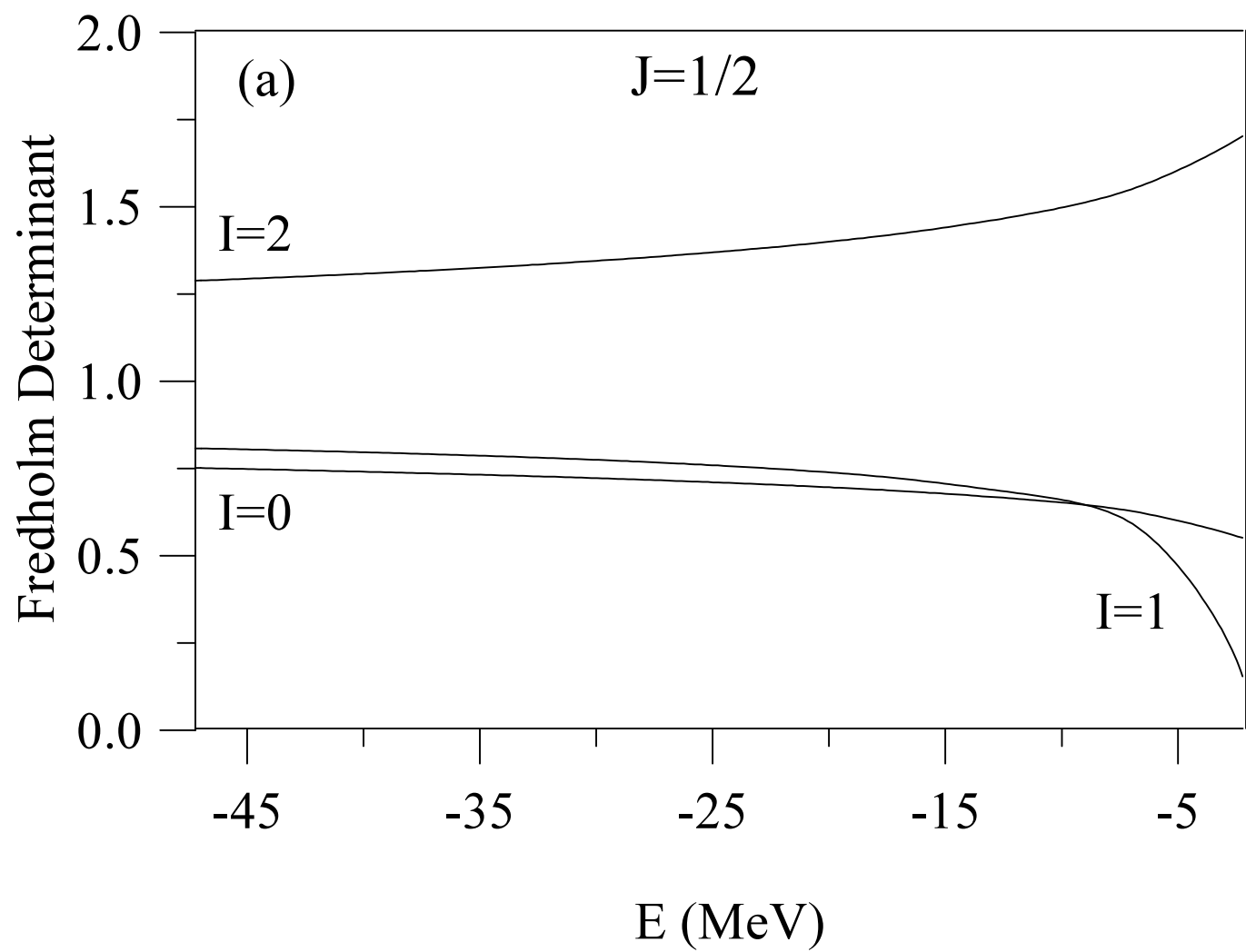


Figure 2

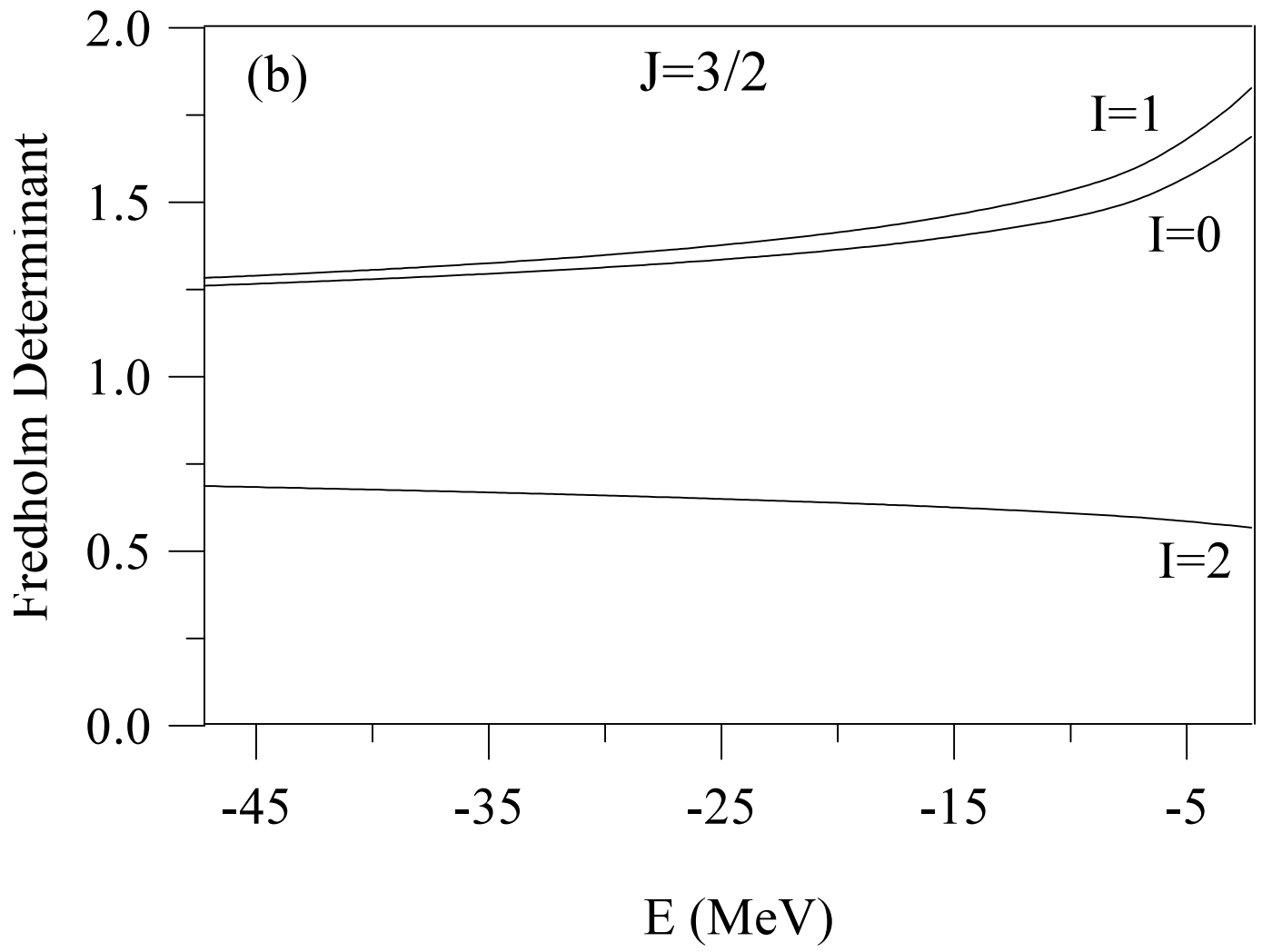


Figure 2

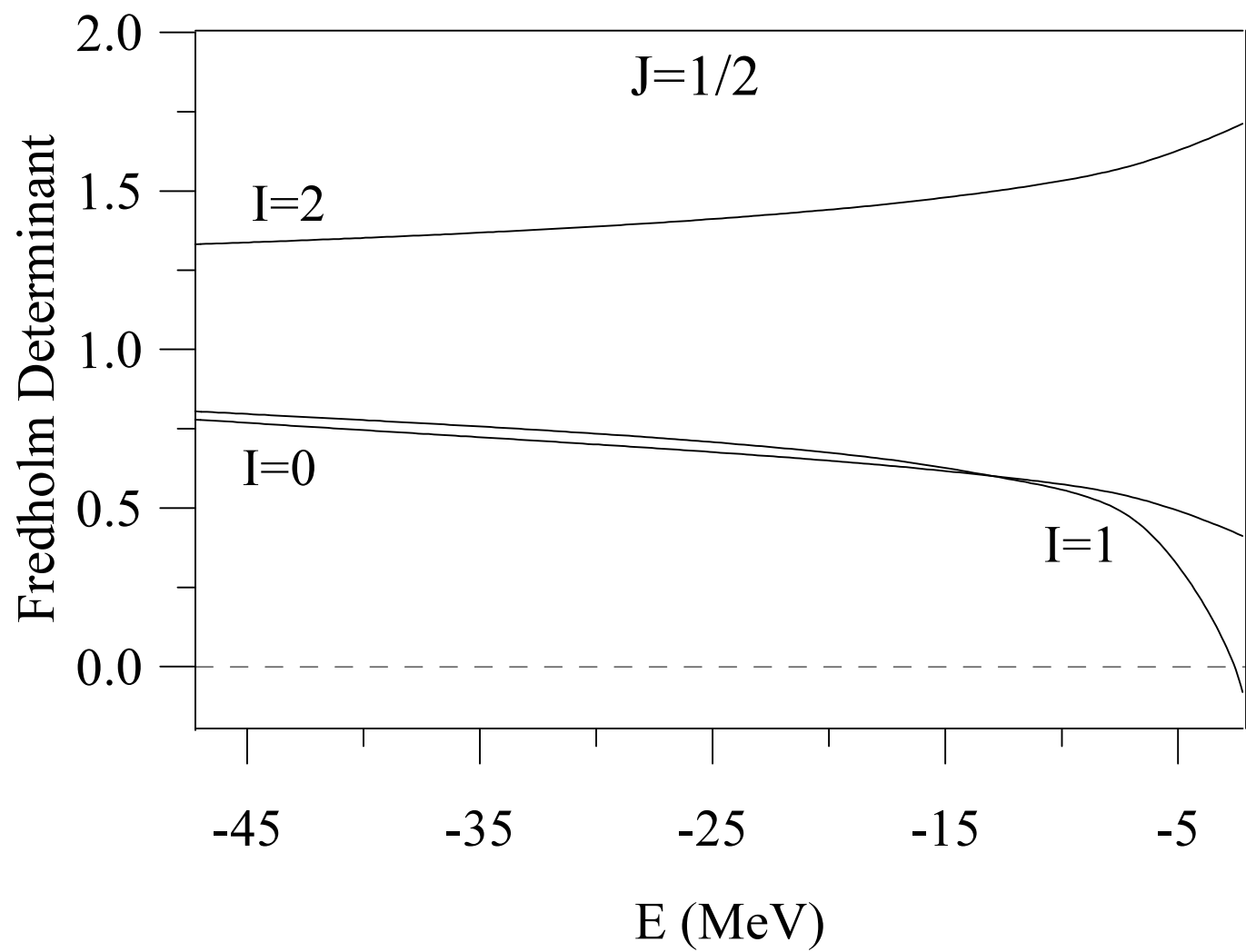


Figure 3

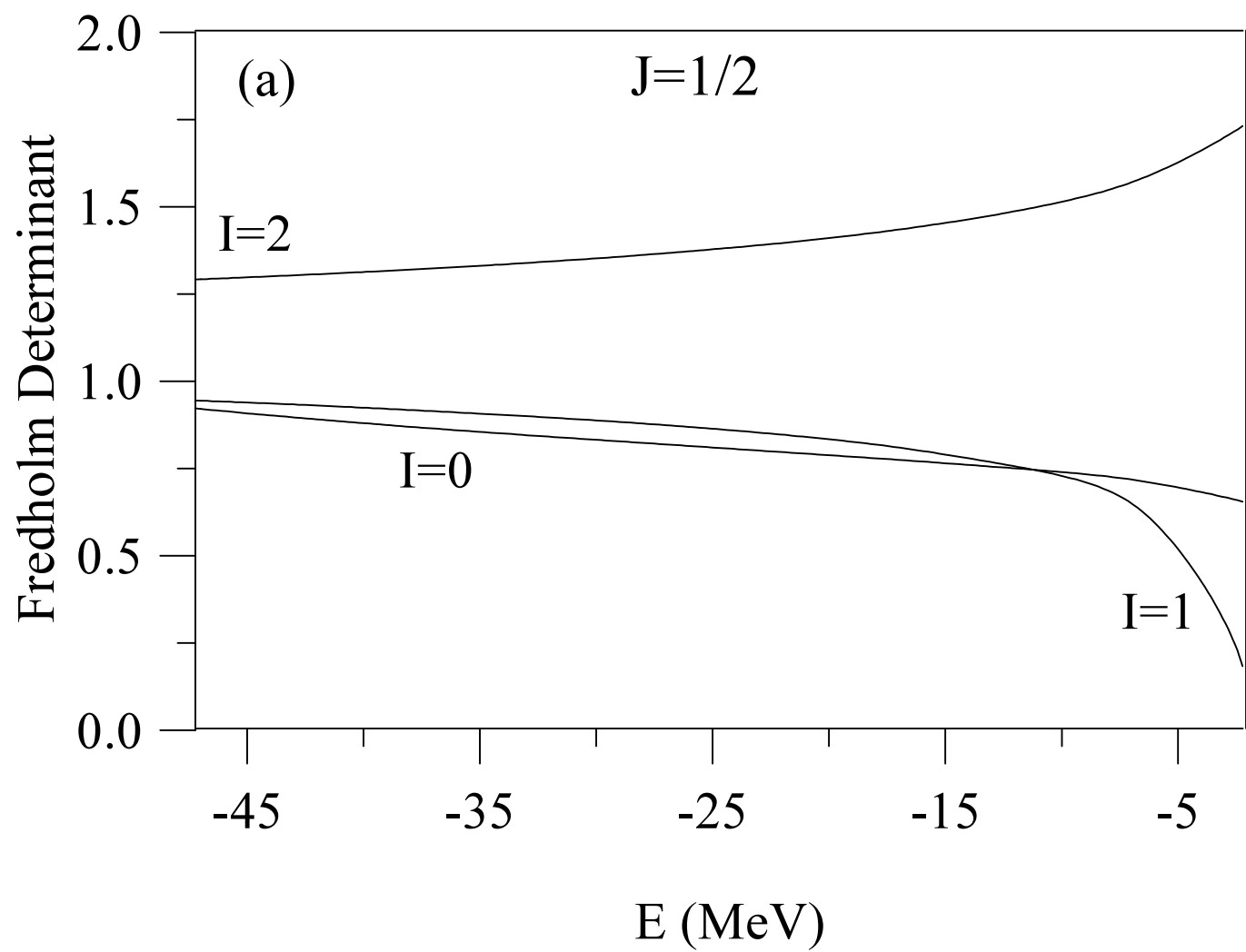


Figure 4

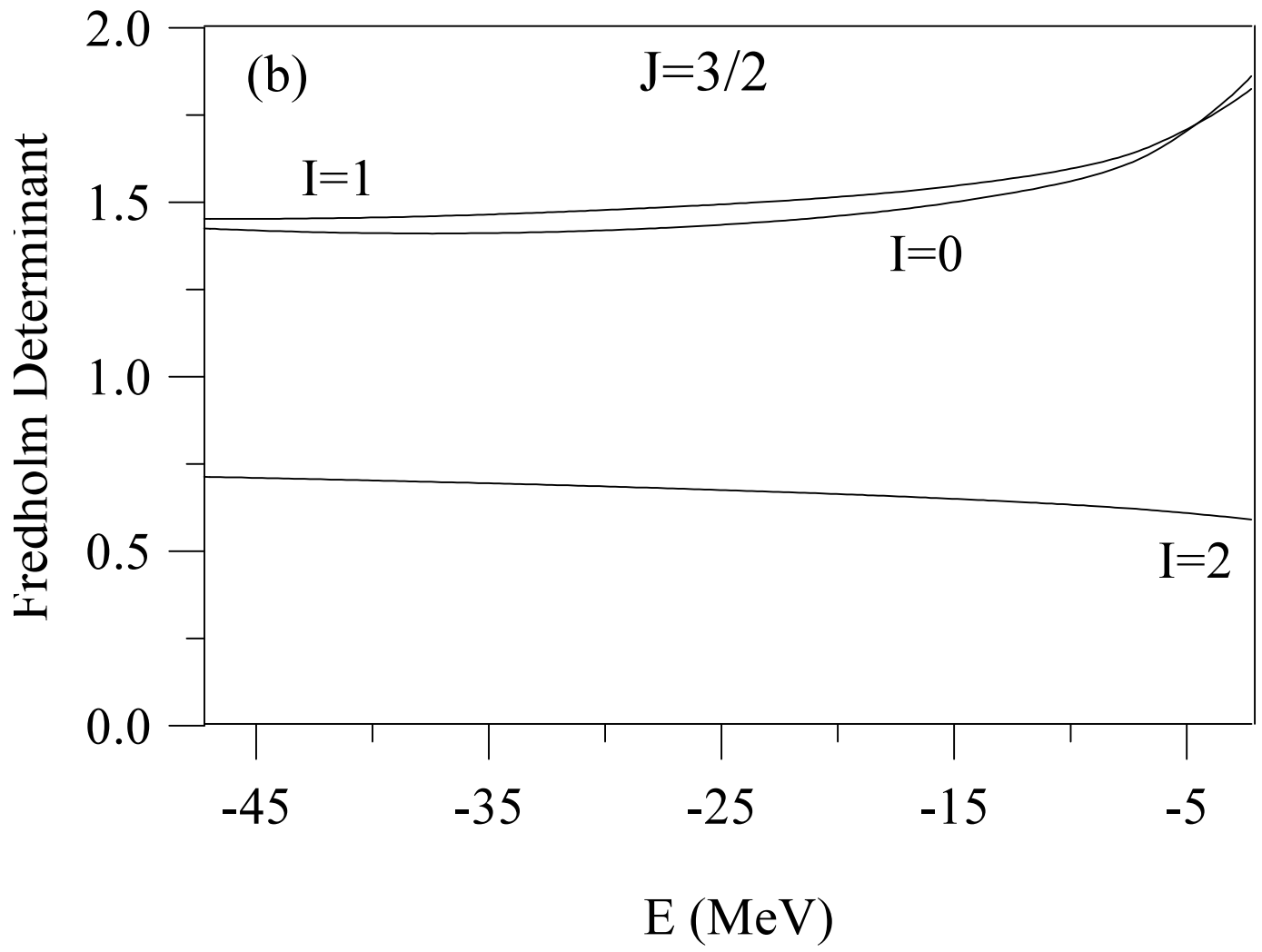


Figure 4

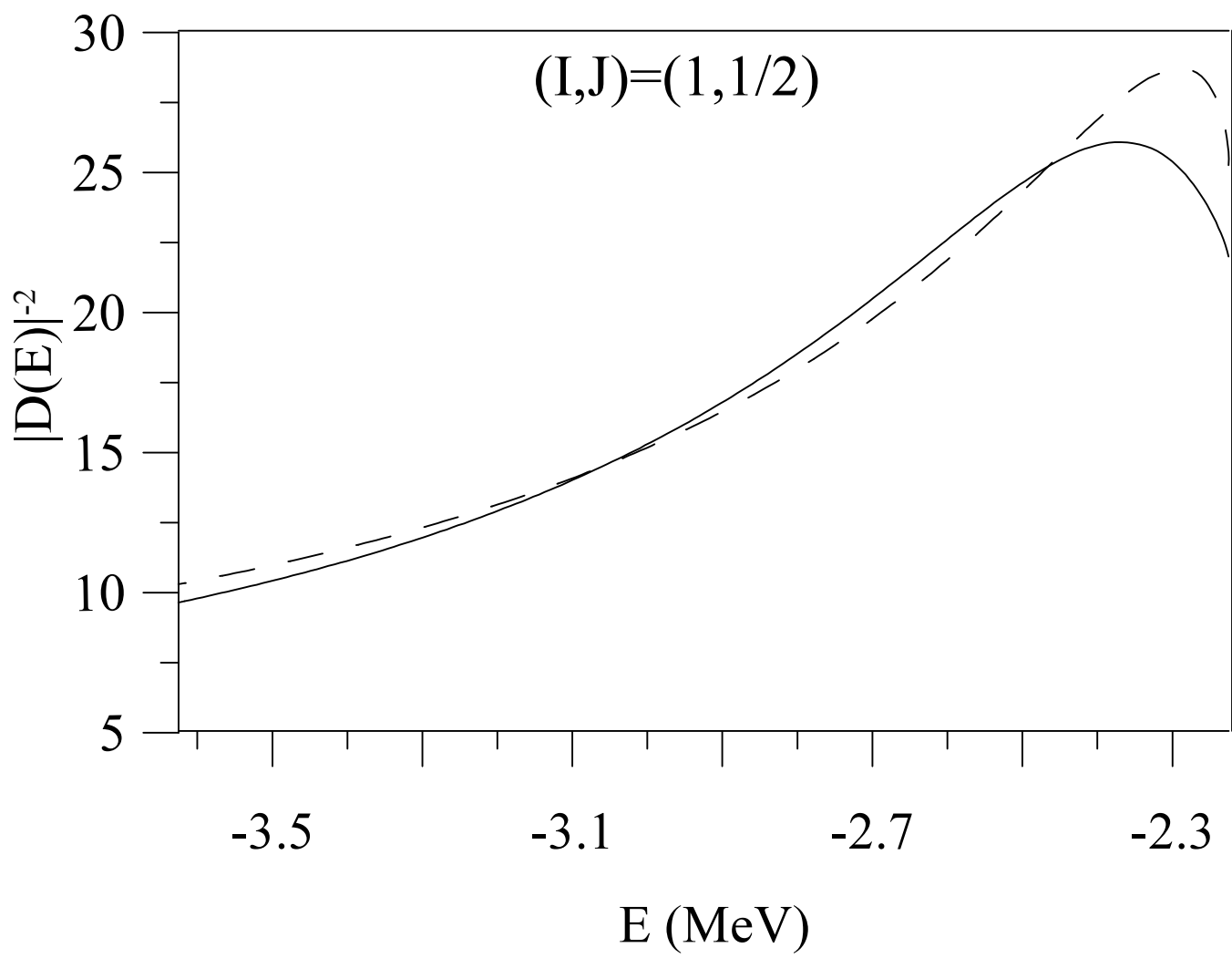


Figure 5